J. Pharm. Pharmacol. 1992, 44: 627–633
Received November 7, 1991

Amorphism and Physicochemical Stability of Spray-dried Frusemide

YOSHIHISA MATSUDA, MAKOTO OTSUKA, MIKA ONOE AND ETSUKO TATSUMI

Department of Pharmaceutical Technology, Kobe Women's College of Pharmacy, Motoyama-Kitamachi 4-19-1, Higashi-Nada, Kobe 658, Japan

Abstract—The physicochemical properties of amorphous forms of frusemide, prepared by spray-drying at 50 or 150°C, and their hygroscopic stability at temperatures of 25 and 40°C, and at 0 and 75% relative humidity were investigated. The glass transition temperature of the amorphous form A was 44·2°C as measured by differential scanning calorimetry, while that of the amorphous form B was 54·4°C. The activation energies for glass transition and crystallization processes were calculated from the differential scanning calorimetry thermograms of amorphous forms A and B, respectively. Stability determined by X-ray diffraction at 0% relative humidity, 25 and 40°C suggested that form B was more stable than form A. However, the stability of form A at 75% relative humidity and 25 and 40°C was similar to that of form B.

The amorphous state may determine bioavailability of a slightly water-soluble drug because this property affects solubility and hence absorption of the drug in the gastrointestinal tract. There are several methods used to prepare amorphous drug solids, including rapid cooling of a drug melt (Fukuoka et al 1987), freeze-drying (Otsuka & Kaneniwa 1983a), spray-drying (Sato et al 1981) and grinding (Otsuka & Kaneniwa 1983b). However, the nature of the amorphous drug obtained by spray-drying has not been well investigated.

Frusemide is widely used as a diuretic, as an antihypertensive, and as a control for evaluating the therapeutic effect of a drug on renal insufficiency (Kingsford et al 1984). In the present study, we have investigated the physicochemical properties and the hygroscopic stability of amorphous frusemide prepared by spray-drying.

Materials and Methods

Materials

A bulk sample of frusemide, JP XI (lot A-013101), was obtained from Shizuoka Caffeine Co. (Shizuoka, Japan).

Preparation of amorphous frusemide

The drug (1 g) was dissolved in 400 mL of chloroform/methanol (4:1) and the solution was fed into a mini-spray-drier (Pulvis Basic Unit, Model GB-21, Yamato Co., Japan) through a peristaltic pump. The temperature at the inlet of the drying chamber was maintained at either 50 or 150°C. The yields of spray-dried products at these temperatures were approximately 20 and 10%, respectively. The weight loss of both spray-dried products obtained at 50 and 150°C were 0·21 and 0·18%, respectively, as determined by thermogravimetry. All assays were performed on fresh samples.

Methods

X-Ray powder diffraction analysis. X-Ray powder diffraction profiles were taken at room temperature (21°C) with an X-ray diffractometer (XD-3A, Shimadzu Co., Japan). The operating conditions were as follows: target, Cu; filter, Ni; voltage 25 kV; current, 10 mA; receiving slit, 0·1 mm; time constant, 1 s; counting range, 1 kHz; scanning speed 1° 2θ min^{-1}.

Measurement of crystallinity. Known quantities of standard mixtures were obtained by physically mixing frusemide form I and the amorphous form reported previously (Matsuda & Tatsumi 1990) at various ratios in a mortar with a spatula. The calibration curve for measuring the crystallinity was based on the peak height ratio of the X-ray diffraction intensity at 24·7° (2θ) of crystalline form I to that at 15·9° attributable to lithium fluoride using the external standard method. The plots showed good linear correlation and were always reproducible as shown in the following regression equation:

$$Y = 0{\cdot}0118\,X - 0{\cdot}024 \qquad (r = 0{\cdot}998,\ n = 6)$$

where Y is the ratio of peak intensity of form I ($2\theta = 24{\cdot}7°$) to that of lithium fluoride ($2\theta = 15{\cdot}9°$) and X is the percent content of form I.

Infrared (IR) spectroscopy. IR spectra were taken by the Nujol mull method on an IR spectrophotometer (type 270-30, Hitachi Co., Japan).

Thermal analysis. Differential scanning calorimetry (DSC) and thermogravimetry were carried out with a type 3100 instrument (Mac Science Co., Japan) and a type TG-30 instrument (Shimadzu Co., Japan), respectively. The operating conditions in an open pan system were as follows: sample weight, 5 mg; heating rate, 10°C min^{-1}; N_2 flow rate, 30 mL min^{-1}.

Scanning electron microscopy. Photographs of samples were taken with a scanning electron microscope (model JSM-T20, Jeol Co., Japan) at a magnification of × 3500.

Kinetic interpretation of glass transition and crystallization of

Correspondence: M. Otsuka, Department of Pharmaceutical Technology, Kobe Women's College of Pharmacy, Motoyama-Kitamachi 4-19-1, Higashi-Nada, Kobe 658, Japan.

frusemide during DSC measurement. The fractional glass transition and crystallization of amorphous frusemide were calculated by measuring latent and crystallization heats, respectively. The kinetic parameters were estimated using the first-order or three-dimensional growth of nuclei (Avrami) equations (Criado et al 1978).

Physicochemical stability of amorphous frusemide at various relative humidities and temperatures. Samples (50 mg) were loaded in a glass holder for X-ray diffraction, and the holder was stored at 0% (P_2O_5) or 75% (saturated aqueous solution of NaCl) relative humidities, at 25 and 40°C in a desiccator. The sample holders were removed from the desiccator at appropriate time intervals to examine the X-ray powder diffraction profiles. The amount transformed was determined by the X-ray powder diffraction method described in the previous section.

Results and Discussion

X-ray diffraction and IR spectra of spray-dried frusemide

Fig. 1 shows the X-ray powder diffraction profiles of spray-dried frusemide. The samples spray-dried at 50 (amorphous form A) and 150°C (amorphous form B) exhibited no diffraction peaks, but instead displayed a halo pattern, indicating that the spray-dried frusemide was amorphous.

Fig. 2 shows the IR spectra of two amorphous forms and stable crystalline form I (Matsuda & Tatsumi 1990). The IR spectrum of frusemide (crystalline powder) has been explained by Doherty & York (1987) as follows: the band at 3401 cm^{-1} is attributable to the N—H stretch vibration of a secondary amine. The bands at 3353 and 3287 cm^{-1} are attributable to the N—H stretch vibration of a sulphona-

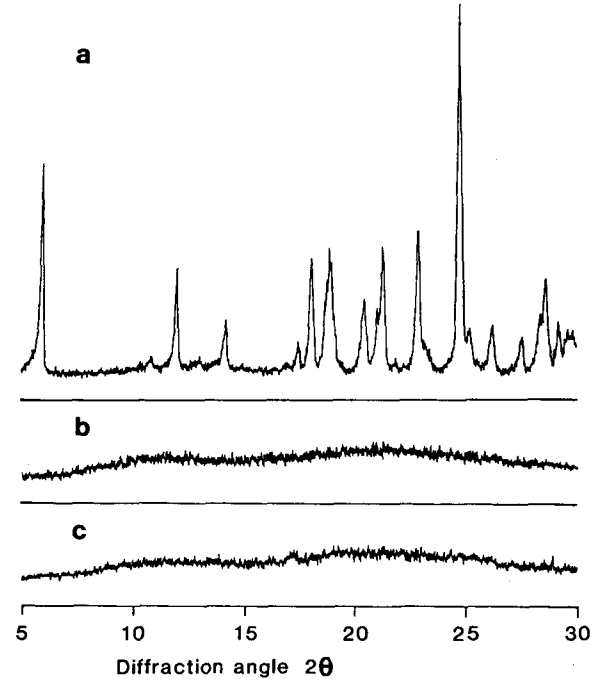

FIG. 1. X-Ray powder diffraction profiles of frusemide modifications. a, form I; b, amorphous A; c, amorphous B.

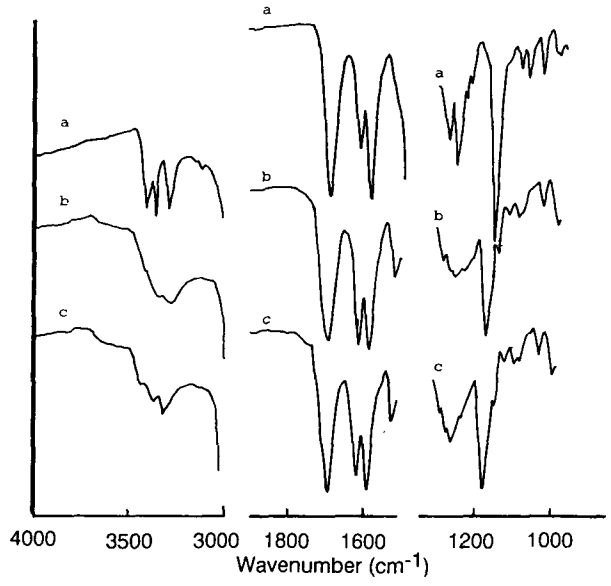

FIG. 2. IR spectra of frusemide modifications. a, form I; b, amorphous A; c, amorphous B.

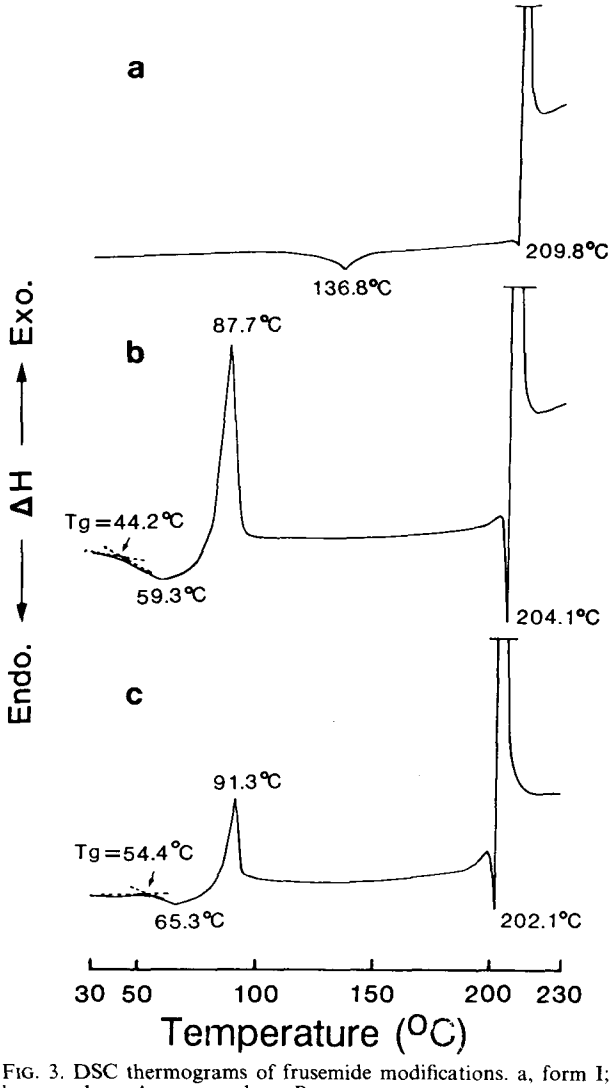

FIG. 3. DSC thermograms of frusemide modifications. a, form I; b, amorphous A; c, amorphous B.

Table 1. Thermodynamic parameters for glass transition and crystallization of two frusemide amorphous forms.

Frusemide form	Glass transition			Crystallization	
	T_g[a] (°C)	E_g[b] (kJ mol^{-1})	H_g[c] (kJ mol^{-1})	E_c[d] (kJ mol^{-1})	H_c[e] (kJ mol^{-1})
Amorphous A	44·2	$1{\cdot}05\times10^{-2}$	5·85	$1{\cdot}14\times10^{-2}$	12·2
Amorphous B	54·2	$2{\cdot}12\times10^{-2}$	0·94	$18{\cdot}4\times10^{-2}$	4·72

[a] Glass transition temperature, [b] activation energy for glass transition, [c] heat of glass transition, [d] activation energy for crystallization, [e] heat of crystallization.

mide group. The bands at 1674 and 1144 cm^{-1} are attributable to the C=O stretch vibration of a carboxyl group and the S=O asymmetric stretch vibration of the sulphonamide group. The S=O bands of the amorphous form B shifted significantly to a higher wavelength (1164 cm^{-1}), whereas none of the N=H absorption peaks changed and the C=O bands slightly widened at 1676 cm^{-1}. The S=O bands of amorphous form A also significantly shifted to a higher wavelength (1166 cm^{-1}), and all N=H absorption peaks became much wider, and the C=O bands also shifted to 1680 cm^{-1}. Lamotte et al (1978) studied the crystal structure using single crystal X-ray diffraction analysis, and concluded that frusemide had two kinds of interhydrogen bonds between the S=O and N—H of the sulphonamide groups, and the C=O and C—OH of the carboxyl groups. Doherty & York (1987) reported the interaction of frusemide-polyvinylpyrrolidone (PVP) solid dispersion by IR spectra, and concluded that frusemide interacted with PVP at the S=O group of sulphonamide. From our IR spectra results and other reports (Lamotte et al 1978; Doherty & York 1987), the molecular states of the amorphous frusemide forms A and B may be considered as follows. Spray-dried amorphous form B contained an inter-molecular hydrogen bond between the carboxyl groups, which was the same as that for crystalline

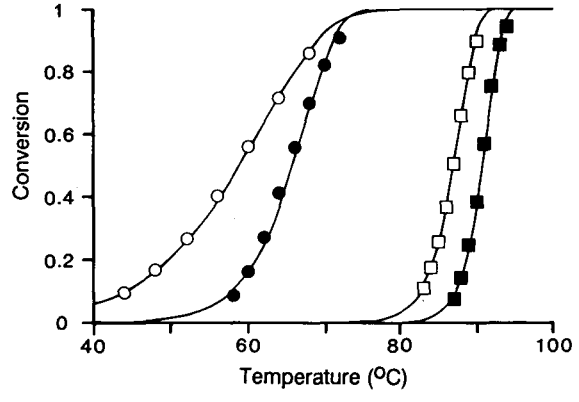

FIG. 4. Glass transition (○, ●) and crystallization (□, ■) processes of amorphous frusemide under nonisothermal conditions. The open and closed symbols represent amorphous A and B, respectively. —— Theoretical curves.

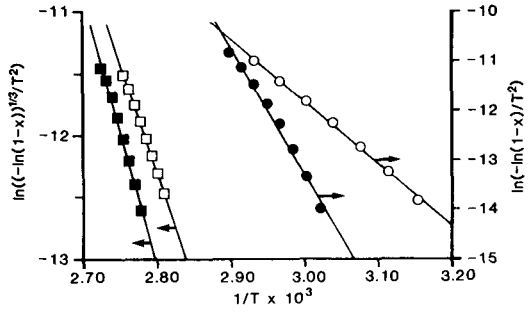

FIG. 5. Criado plots for glass transition (○, ●) and crystallization (□, ■) of amorphous A and B. The open and closed symbols represent amorphous A and B, respectively.

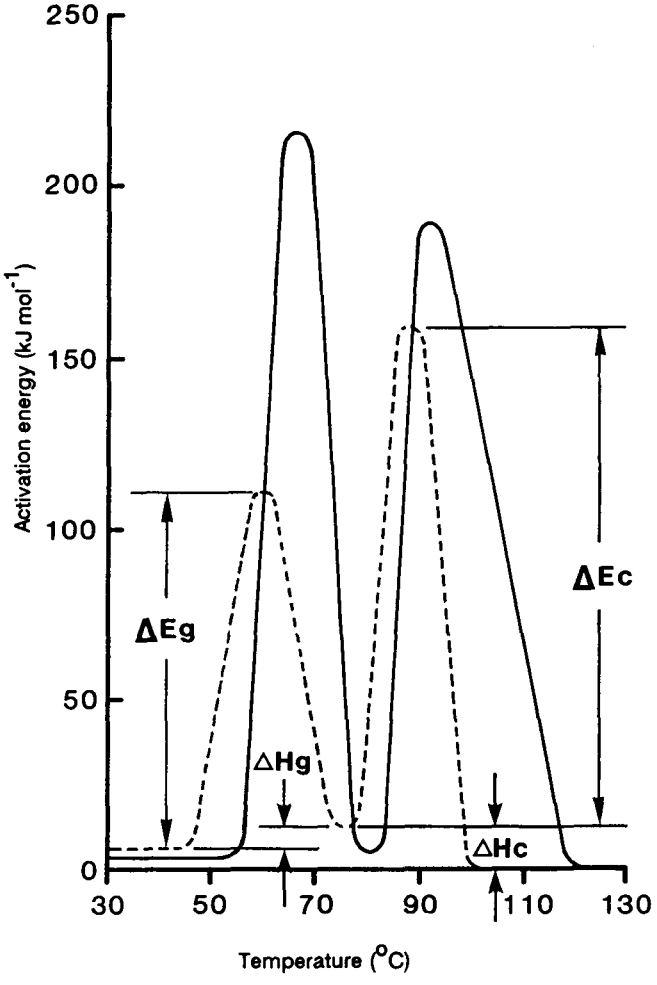

FIG. 6. Schematic diagram of activation energy for glass transition and crystallization of amorphous A (– – –) and B (——). ΔE_g, activation energy for glass transition; ΔE_c, activation energy for crystallization; ΔH_g, heat of glass transition; ΔH_c, heat of crystallization.

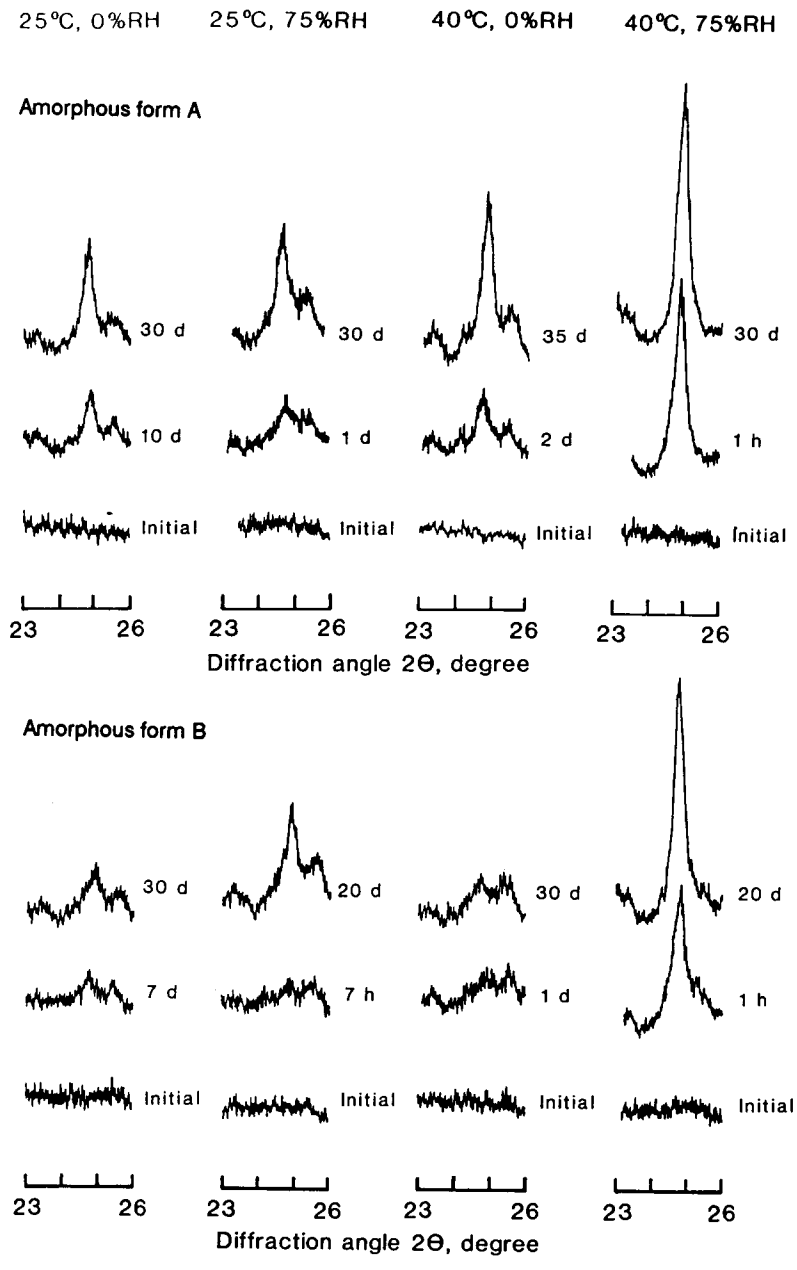

FIG. 7. Effect of relative humidity and temperature on X-ray powder diffraction profiles of amorphous A and B frusemide.

form I. However, there was no interaction between the S=O of the sulphonamide groups, and the molecules were packed in the solid in a noncrystalline state; neither the sulphonamide groups nor the carboxyl groups of amorphous form A formed interhydrogen bonds, and therefore, the molecular packing in a noncrystalline state was different from that of amorphous form B.

The effect of spray-drying temperature on the stability of amorphous frusemide under nonisothermal conditions

Fig. 3 shows the DSC thermograms of the amorphous forms of frusemide. The DSC curve of crystalline form I showed an endothermic peak at 136·8°C attributable to transformation to form IV and the subsequent endo-exothermic peaks at 209·8°C due to decomposition after melting.

The DSC curves of the amorphous forms A and B showed endothermic and exothermic peaks at 40–100°C and second endo- and exothermic peaks at 200–210°C, respectively. The X-ray diffraction patterns obtained for amorphous forms A and B maintained at 150°C for 10 min were identical to that of crystalline form IV since the patterns had the peaks at $2\theta = 18{\cdot}5$, 21·8 and 24·5° attributable to form IV. These findings suggested that the first endothermic peak at 40–70°C was due to glass transition, that the first exothermic peak at 80–100°C was due to crystallization of crystalline form IV which was stable above 136·8°C, and that the second endo- and exothermic peaks at 200–210°C were due to decomposition after melting. The results of thermal X-ray diffraction analysis suggest that these amorphous forms had transformed to form IV after crystallization, and the sample was

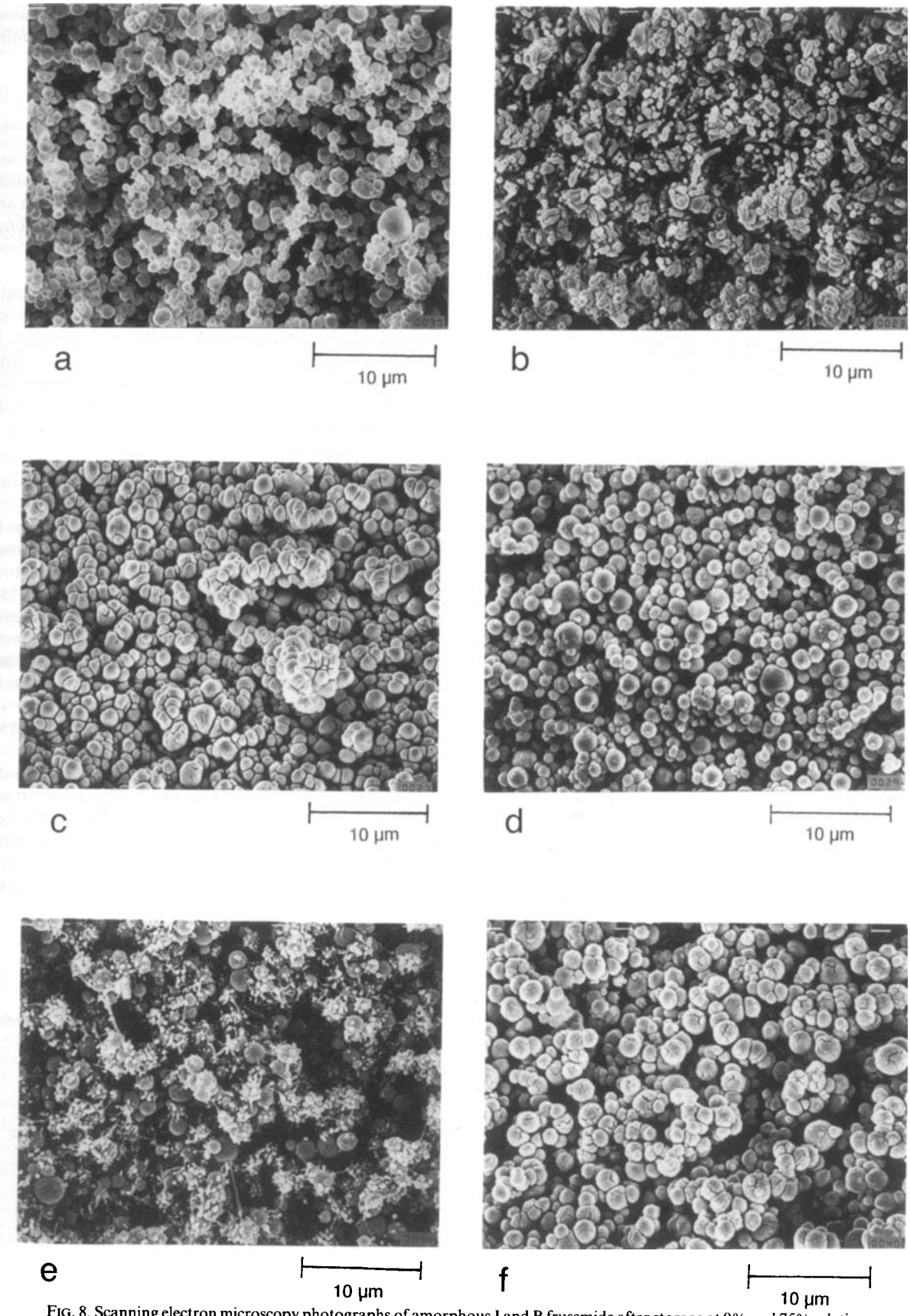

FIG. 8. Scanning electron microscopy photographs of amorphous I and B frusemide after storage at 0% and 75% relative humidity, 40°C. (a, d), intact; (b, e), at 0% humidity for 5 days; (c, f), at 75% humidity for 5 days; (a, b, c), amorphous A; (d, e, f), amorphous B.

transformed into crystalline form I after cooling at 25°C. The transformation pathway of amorphous forms under non-isothermal conditions can be obtained as follows:

$$\text{amorphous} \xrightarrow[E_g,\ H_g]{T_g \text{ relaxation}} \text{super cooling liquid} \xrightarrow[E_c,\ H_c]{\text{nucleation and crystal growth}} \text{crystal form IV}$$

where, T_g is glass transition temperature, E_g is activation energy for glass transition, H_g is heat of glass transition, E_c is activation energy for crystallization and H_c is heat of crystallization.

The T_g of amorphous form A was 44·2°C, while that of amorphous form B was 54·4°C. This indicates that the latter is more stable than the former at room temperature. The heat of the glass transition of amorphous form A was 6 times higher than that of amorphous form B. The H_c of the amorphous form A was 2·58 times higher than that of the amorphous form B as shown in Table 1.

Fig. 4 shows the glass transition and crystallization processes of amorphous frusemide estimated from an anomalous endothermic peak, H_g, at 30–80°C and an exothermic peak, H_c, at 80–100°C, respectively. Criado et al (1978) derived equation 1 from the Arrhenius equation and nine solid-state kinetic equations, g(x):

$$\ln (g(x)/T^2) = \ln (AR/QE) - E/R \quad (1)$$

where x is the fractional conversion at time t, T is temperature, R is the gas constant, A is the frequency factor, Q is the heating rate and E is activation energy.

Barton (1969) reported that the time dependence of transformation from a glass to a liquid state can be treated as a good approximation of a first-order kinetic process with a relaxation time. Therefore, the kinetic parameters were estimated based on the first-order kinetic equation (eqn 2). It was also assumed that the crystallization process followed a three-dimensional growth of nuclei equation (Avrami eqn (Criado et al 1978)) (eqn 3) since the shape of spray-dried products was spherical and the start of the transformation was random as determined by observation of the scanning electron microscopy photographs after heating.

$$g(x) = -\ln (1-x) \quad (2)$$

$$g(x) = (-\ln (1-x))^{1/3} \quad (3)$$

Fig. 5 shows the Criado plots for glass transition and crystallization processes of amorphous frusemide under nonisothermal conditions. The plots for glass transition and crystallization are straight lines for both amorphous forms (A and B). The kinetic parameters, E_g and E_c, calculated from the slopes are summarized in Table 1.

Fig. 6 demonstrates the schematic diagram of thermodynamic stability of amorphous frusemide. The chemical potentials of amorphous forms A and B were estimated to be 6·35 and 3·78 kJ mol^{-1}, respectively, from the thermodynamic parameter. The results of the chemical potential suggested that the amorphous form B was more stable than the amorphous form A.

Effect of relative humidity and temperature on the physicochemical stability of amorphous frusemide

Fig. 7 shows the effect of environmental conditions on the X-ray diffraction profiles of amorphous frusemide. All intact spray-dried samples showed the halo pattern in X-ray powder diffraction profiles, but after storage at 0 and 75% humidity, at 25 and 40°C, samples showed X-ray diffraction profiles with peaks attributable to stable crystalline form I (Matsuda & Tatsumi 1990). The results indicated that amorphous form B was more stable than the amorphous form A under the investigated conditions, and that the amorphous forms were more stable at 0 than at 75% humidity, and at 25 than at 40°C.

Fig. 8 shows the scanning electron microscopy photographs of amorphous forms A and B after storage at 0 and 75% humidity, 40°C. The amorphous forms A and B were spherical particles of 1–3 μm in diameter. After storage at 0% humidity for 5 days, amorphous forms A and B had many whiskers on their surfaces. The diameter of whiskers on the

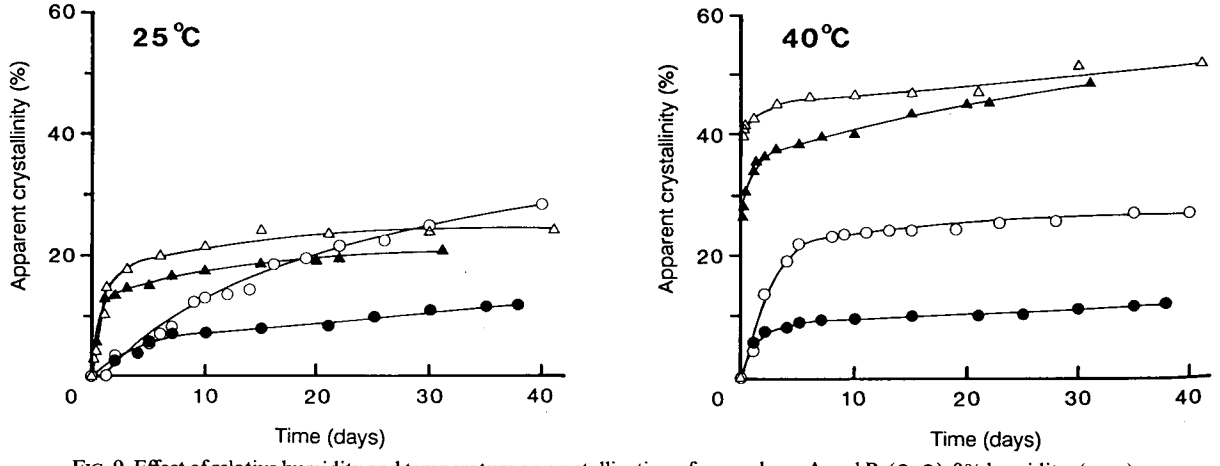

FIG. 9. Effect of relative humidity and temperature on crystallization of amorphous A and B. (○, ●), 0% humidity; (△, ▲), 75% humidity. The open and closed symbols represent amorphous A and B frusemide, respectively.

Table 2. Effect of storage conditions on the initial crystallization rate constant (ICR) of amorphous frusemide.

Sample	Temperature (°C)	ICR (day^{-1}) 0% humidity	75% humidity
Amorphous A	25	$1{\cdot}46 \times 10^{-2}$	$1{\cdot}14 \times 10^{-1}$
Amorphous A	40	$5{\cdot}02 \times 10^{-2}$	6·44
Amorphous B	25	$7{\cdot}86 \times 10^{-3}$	$6{\cdot}90 \times 10^{-2}$
Amorphous B	40	$3{\cdot}98 \times 10^{-2}$	2·32

The ICR values were estimated from Fig. 9 based on the first-order kinetics.

surface of amorphous form A was larger than that on the amorphous form B. After storage at 75% humidity for 5 days the amorphous forms A and B were converted to round particles with grooves. This suggests that the particles were covered with transformed fine crystals of crystalline form I from the surface of the particles.

Fig. 9 shows a change in the apparent crystallinity of amorphous frusemide at 0 and 75% humidity and at 25 and 40°C. The apparent crystallinity of the amorphous forms A and B markedly increased within the first few days, and thereafter the crystallinity increased very slowly even when stored for over 10 days. At 40°C, 75% humidity, amorphous forms A and B had crystallinity values of 45% over 40 days storage, while at 0% humidity the former was 23% and the latter was 10%. On the other hand, at 25°C, 75% humidity, amorphous forms A and B had crystallinity of 19 and 22% over 40 days storage, respectively, but at 0% the former had 15% and the latter only 8%. Since the storage temperatures investigated were lower than the T_g of both amorphous forms, the crystals did not grow from a super cooled liquid, but directly from the amorphous forms. The stability test at 0% humidity (Table 2) suggested that the amorphous form B was more stable than amorphous form A, and supported the result of the chemical potentials described previously. However, the stability of amorphous form A at 75% humidity (Table 2) was almost the same as that of amorphous form B, and did not support the results of the nonisothermal study. Otsuka & Kaneniwa (1983a) reported that the hygroscopicity of freeze-dried amorphous cephalexin, as well as the amorphous form, was very unstable at high humidity. It can be concluded that the amorphous form B is more stable than the amorphous form A at low humidity, and both amorphous forms were unstable under conditions of high humidity.

References

Barton, J. M. (1969) Dependence of polymer glass transition temperature on heating rate. Polymer 10: 151–154

Criado, J. M., Morales, J., Rives, V. (1978) Computer kinetics analysis of simultaneously obtained TG and DTG curves. J. Therm. Anal. 14: 221–228

Doherty, C., York, P. (1987) Evidence for solid- and liquid-state interactions in a furosemide-polyvinylpyrrolidone solid dispersion. J. Pharm. Sci. 76: 731–737

Fukuoka, E., Makita, M., Yamamura, S. (1987) Glassy state of pharmaceuticals. II. Bioinequivalence of glassy and crystalline indomethacin. Chem. Pharm. Bull. 35: 2943–2948

Kingsford, M., Eggers, N. J., Soteros, G., Maling, T. J. B., Shirkey, R. J. (1984) An in-vivo–in-vitro correlation for the bioavailability of frusemide tablets. J. Pharm. Pharmacol. 36: 536–538

Lamotte, J., Campsteyn, H., Dupont, L., Vermeire, M. (1978) Structure crystalline et moleculaire del'lacide furfurylamino 2-chloro-4 sulfamolyl-5-benzoique, la furosemide ($C_{12}H_{11}ClN_2O_5S$). Acta Cryst. B34: 1654–1661

Matsuda, Y., Tatsumi, E. (1990) Physicochemical characterization of furosemide modifications. Int. J. Pharm. 60: 11–26

Otsuka, M., Kaneniwa, N. (1983a) Hygroscopicity and solubility of noncrystalline cephalexin. Chem. Pharm. Bull. 31: 230–236

Otsuka, M., Kaneniwa, N. (1983b) Effect of grinding on the degree of crystallinity of cephalexin powder. Ibid. 31: 4489–4495

Sato, T., Okada, A., Sekiguchi, K., Tsuda, Y. (1981) Difference in physico-pharmaceutical properties between crystalline and non-crystalline 9, 3″-diacetylmidecamycin. Ibid. 29: 2675–2682